Biochemical and Biophysical Research Communications **281,** 212–219 (2001)
doi:10.1006/bbrc.2001.4335, available online at http://www.idealibrary.com on IDEAL®

A Novel Host Cell Reactivation Assay to Assess Homologous Recombination Capacity in Human Cancer Cell Lines

Robbert J. C. Slebos*,[1] and Jack A. Taylor*,†
**Laboratory of Molecular Carcinogenesis and †Epidemiology Branch, National Institute of Environmental Health Sciences, Research Triangle Park, North Carolina 27709*

Received January 11, 2001

Repair of DNA double-strand breaks (DSB) is essential for cell viability and genome stability. Homologous recombination repair plays an important role in DSB repair and impairment of this repair mechanism may lead to loss of genomic integrity, which is one of the hallmarks of cancer. Recent research has shown that the tumor suppressor genes p53 and BRCA1 and -2 are involved in the proper control of homologous recombination, suggesting a role of this type of repair in human cancer. We developed a novel assay based on recombination between two Green Fluorescent Protein (GFP) sequences in transiently transfected plasmid DNA. The plasmid construct contains an intact, emission-shifted, "blue" variant of GFP (BFP), with a 300 nucleotide stretch of homology to a nonfunctional copy of GFP. In the absence of homologous recombination only BFP is present, but homologous recombination can create a functional GFP. The homologous regions in the plasmid were constructed in both the direct and the inverted orientation of transcription to detect possible differences in the recombination mechanisms involved. A panel of human tumor cell lines was chosen on the basis of genetic background and chromosome integrity and tested for homologous recombination using this assay. The panel included cell lines with varying levels of karyotypic abnormalities, isogenic cell lines with normal and mutant p53, isogenic cell lines with or without DNA mismatch repair, BRCA1 and -2 mutant cell lines, and the lymphoma cell line DT40. With this assay, the observed differences between cell lines with the lowest and highest levels of recombination were about 100-fold. Increased levels of recombination were associated with mutant p53, whereas a low level of recombination was found in the BRCA1 mutant cell line. In the cell line HT1080TG, a mutagenized derivative of HT1080 with two mutant alleles of p53, high levels of recombination were found with the direct orientation but not with the inverted orientation plasmid. No difference in recombination was detected between two isogenic cell lines that only differed in DNA mismatch repair capability. We conclude that this assay can detect differences in homologous recombination capacity in cultured cell lines and that these differences follow the patterns that would be expected from the different genotypes of these cell lines. Future application in normal cells may be useful to identify genetic determinants controlling genomic integrity or to detect differences in DNA repair capacity in individuals.

Key Words: **homologous recombination; green fluorescent protein; host cell reactivation assay.**

Abbreviations used: HR, homologous recombination; GFP, green fluorescent protein; BFP, blue fluorescent protein; nm, nanometer.

[1] To whom correspondence should be addressed at National Institute of Environmental Health Sciences, Laboratory of Molecular Carcinogenesis, Maildrop C2-01, P.O. Box 12233, Research Triangle Park, NC 27709. Fax: 919-541-2511. E-mail: slebos@niehs.nih.gov.

Loss of genomic integrity is a common feature found in almost all human cancers (for reviews see (1, 2)). Whether this ubiquitous phenotype is a necessary step in tumorigenesis has long been debated, but recent evidence indicates that several pathways involved in the maintenance of genomic integrity are altered in human tumors. Genomic instability can be manifest either at the nucleotide level or at the chromosomal level. An example of instability at the nucleotide level can be found in hereditary non-polyposis colorectal cancer (HNPCC) where defects in mismatch repair genes cause widespread genetic mutation. Chromosomal level instability, leading to aneuploidy, can be found in almost all other tumors. Chromosomal abnormalities can occur as a result of DNA double-strand breaks (DSBs) that are not properly repaired (3). When a cell is not capable of repairing a DSB but continues to divide, the broken chromosome fragments will missegregate and/or degrade, resulting in aneuploidy. Generally, DSBs can be repaired by two competing

0006-291X/01 $35.00

mechanisms: non-homologous end-joining (NHEJ) and homologous recombination (HR). Defective NHEJ is associated with increased sensitivity to ionizing radiation and genomic instability (4, 5). Currently, there is only limited evidence that defects in NHEJ contribute to human cancer. The importance of HR in the maintenance of genomic integrity is becoming increasingly clear (3, 6). It was recently shown that in mammalian cells, about half of all DSBs are repaired by mechanisms involving HR (7). Much of our understanding of the genes involved in HR comes from studies in the yeast *Saccharomyces cerevisiae,* where the products of the RAD51, 52, 54 and other genes are responsible for the observed high levels of HR (8).

Several inherited syndromes that are associated with an increased risk for cancer involve genes that are essential for repair of DNA double-strand breaks. Examples of these rare genetic instability disorders with an increased incidence of cancer include Nijmegen Breakage Syndrome (NBS), Bloom's Syndrome (BS), Ataxia Telangectasia (AT), and Fanconi Anemia (FA) (1). Further evidence for a link between cancer development and DSB repair comes from studies on the two inherited breast cancer tumor suppressor genes BRCA1 and BRCA2 (for review see (9)), and from the p53 tumor suppressor gene (10, 11). BRCA2 directly binds to Rad51, while BRCA1 colocalizes with Rad51 after DNA damage, and both proteins are necessary for homologous recombination in mammalian cells (12, 13). A functional p53 tumor suppressor gene is required for the maintenance of genomic stability, a function that may be related to its role in HR (10, 11, 14). Cells with mutant p53 have greatly increased levels of HR, a function that is separate from p53 transactivation or G1/S cell cycle control (15, 16). In addition, there is now evidence for physical and functional interactions between p53, Rad51 and BRCA2, which suggest interplay of these proteins in the maintenance of genomic integrity (17, 18). Further evidence for the importance of HR in cancer development comes from the observation that human homologues of Rad54 harbor somatic mutations in some human cancers (19, 20).

Early observations of HR in mammalian cells were performed using a plasmid rescue system with truncated *neo* gene sequences (21). This system measures homologous recombination between two inactive copies of the *neo* gene followed by successful integration into the host genome. A different model system makes use of homologous recombination between SV40 sequences upon infection, followed by rescue of the virus in the viral plaque assay (22). A similar approach was used in a study where plasmid HR was measured in primate cell lines by isolation of extrachromosomal DNA and measuring the number of recombination events by transformation of *Escherichia coli* (23). All of these methods require multiple steps involving plasmid integration into the genome, plasmid rescue from the cells, or coexpression of proteins that affect homologous recombination (SV40 Large T antigen).

In this paper we describe the development of a novel host-cell reactivation assay to directly measure the levels of homologous recombination using flow cytometric determination of Green Fluorescent Protein (GFP) as our endpoint. To validate the assay, we obtained estimates for homologous recombination in a panel of human tumor cell lines with known defects in DNA repair genes. We demonstrate that the assay can detect the differences caused by genes involved in homologous DNA repair (p53 and BRCA1).

MATERIALS AND METHODS

Cell lines and growth conditions. The following human cell lines were used in this study: colorectal carcinoma RKO, HCT116, and HCT116+3, lung carcinoma A549, Calu-1, NCI-H661 and NCI-H520, fibrosarcoma HT1080 and HT1080TG, osteosarcoma Saos-2 and G292, breast carcinoma HCC1937, pancreas carcinoma Capan-1, and the chicken lymphoma cell line DT40. RKO and HCT116 are mismatch repair deficient cell lines. HCT116+3 is a derivative of HCT116 in which mismatch repair has been restored by chromosome transfer (24). HT1080TG is a derivative of HT1080 obtained by thio-guanine mutagenesis. HT1080 is wild-type for p53, while HT1080TG has two independent mutations in each of the p53 alleles (25). All cell lines were obtained from ATCC, except for the HCT116 and DT40 lines which were provided by Dr. Koi, and HT1080TG which was provided by Dr. Risinger. Cell lines were grown in DMEM/F12 (RKO, A549, and the HCT116 lines), EMEM (HT1080 lines), McCoy5A (Calu-1, G292, and Saos-2), and RPMI (HCC1937, Capan-1, H520 and H661) supplemented with 10% fetal bovine serum and penicillin/streptomycin. DT40 was grown in modified DMEM as described previously (26).

Cloning of plasmid vectors. The first step in the cloning procedure was to generate a blue shifted version of pHygEGFP by replacing the BseRI-NotI fragment from pHygEGFP, containing almost full length EGFP, by the BseRI-NotI fragment of pEBFP-N1 (both from Clontech, Palo Alto, CA). The resulting construct, pHygEBFP was tested and shown to encode a functional blue-shifted GFP (data not shown). The next step was to generate a chimeric GFP by combining the 5′ end of wild-type *Aequorea victoria* GFP and the 5′ end of Enhanced ("humanized") GFP (EGFP). EGFP was originally made by introducing mutations in the wild-type GFP sequence to reflect human codon usage and to increase the fluorescent properties of the fluorochrome. The humanized GFP sequence is only 70% homologous to the wild-type GFP sequence, a level that is too low to drive homologous recombination. The 5′ sequence of wild-type GFP, fragment GB, was PCR amplified from plasmid pGFPmut3.1 (Clontech, Palo Alto, CA) using primers GS-S (5′-CAA CTA GCT AGC GCC ACC ATG *A*GT AAA GGA GAA GAA CTT-3′) and GM-AS (5′-CGA AAC GCT CCA TGG GTC TA-3′). The proofreading thermostable *Pfu* polymerase (Stratagene, CA) was used for a 10-cycle PCR to reduce the chance of amplification-induced mutations. The primer GS-S contains a NheI restriction site, a Kozak translation initiation consensus sequence and the ATG protein translation start codon. The primer GM-AS is located downstream of the chromophore-encoding area of GFP (codons 64 to 66) and contains an artificial KpnI restriction site that does not alter the protein sequence. Two PCR fragments were generated from the 3′ part of EGFP: the first, PR, encodes the remaining part of the protein (codons 66 to 239) and a second, TR, that was predicted to encode a carboxy-terminally truncated EGFP protein (codons 66 to 178). The fragment PR was generated using primers GSE-S (5′-TCA GCC GGT ACC CCG ACC ACA TG-3′), which has the same silent artificial KpnI restriction site, and

PR-AS (5′-CGT ACC TGC TCG ACA TGT TCA TCA GAT CTG C-3′). The fragment TR was generated using primers GSE-S and TR-AS (5′-G TA GCT CCT GCC GTC GCA CAT CAG ATC TGC-3′) for the truncated EGFP. Both PR-AS and TR-AS primers encode a XbaI restriction site. After PCR amplification, fragments GB, PR and TR were digested with KpnI and the combination of GB/PR and GB/TR were ligated to form the chimeric full-length and truncated fragments, respectively. Subsequently, these fragments were digested with NheI and XbaI and ligated in the vector pRL-SV40 (Promega, Madison, WI) from which the NheI-XbaI fragment was removed. The pRL-SV40 vector provides SV40 promoter/enhancer and polyadenylation signals to allow eukaryotic expression of the chimeric GFP. The resulting vectors were tested for transient expression of a functional GFP by flow cytometry. The full-length chimeric GFP did result in green fluorescing cells but the truncated chimeric GFP did not (data not shown). The truncated chimeric GFP cassette was then excised from pRL-SV40 by digestion with BglII and BamHI, and ligated into the BglII site of pHygEBFP. Both orientations of the resulting construct were isolated and named pBHRF (forward) and pBHRR (reverse). In pBHRF the orientation of the truncated chimeric GFP and HygEBFP are the same, while in pBHRR they have the opposite orientation of transcription. The mechanisms of intra-plasmid HR will be different as a result of this orientation of the recombination partners, as only the direct orientation would be expected to support recombination as a result of single-strand annealing or replication slippage. As a control plasmid, the full length chimeric GFP was cloned into pHygEBFP to create pHBPR containing intact green and blue fluorescent protein sequences.

Cell transfections and flow cytometry. For each transfection experiment, cells were seeded in 6-well plates and transfected with the plasmid recombination constructs 24 h later. The highest transfection efficiencies were obtained with Lipofectamine 2000 (Life Technologies, Rockville, MD) using conditions as recommended by the manufacturer. For each transfection, 500 ng of plasmid DNA was combined with 5 μl of Lipofectamine 2000 in 0.5 ml Optimem (Life Technologies, Rockville, MD) and incubated for 15 min. This mixture was then added to each well containing 2 ml of Optimem and incubated for 24 h at 37°C. For each 6-well plate, transfections of pBHRF and pBHRR were carried out in duplicate, with pHBPR and a mock transfection in the remaining two wells. Subsequently, the cells were harvested and 50,000–100,000 cells were analyzed by flow cytometry using a FACSVantage SE (Becton Dickinson, San Jose, CA). Green and blue fluorescence were simultaneously examined by exciting the cells using a 488 nm Argon laser (EGFP) and a UV (350–360 nm) laser (EBFP). Green and blue emissions were detected at 530 nm and 424 nm, respectively, while orange fluorescence (575 nm) was measured as an internal standard. Those experiments where the transfection efficiency was below 0.1% were excluded from further analysis. This percentage translates to less than 100 blue fluorescing cells per flow cytometric analysis. For each experiment, green and blue fluorescence signals were plotted against the orange fluorescence signal, GFP and BFP negative cells fall along the orange/green or orange/blue diagonal, while positive cells appear shifted from this diagonal (27). With this detection method, the background green and blue fluorescence signals in untransfected cells are below 0.01% of the signals in plasmid transfected cells. For each individual well, the percentages of green and blue fluorescent cells in the total cell population were used to calculate a green/blue ratio. The average and standard errors of these green/blue ratios were calculated from between four and ten independent wells in separate experiments.

Statistical analyses. All comparisons between green/blue ratios were done on log-normal transformed data using Student's *t*-test assuming equal variance. Alpha values of less than 0.05 were considered statistically significant.

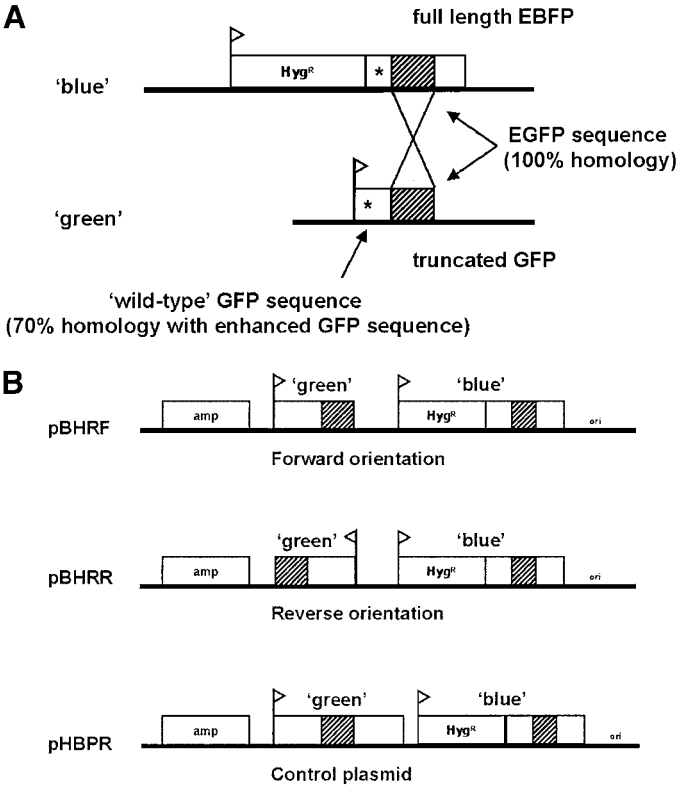

FIG. 1. (A) Recombination between two 300-bp identical sequences of "humanized" EGFP can restore a truncated form of GFP. The intact recombination partner contains a full-length EBFP sequence, which differs from EGFP in only one amino acid position (indicated by *). A wild-type GFP sequence is cloned upstream of the 300-bp homologous sequence, which determines the green fluorescence but is not sufficiently homologous to EGFP to affect recombination. (B) Schematic representation of the plasmid constructs used in this study. The recombination partners EBFP and the chimeric truncated GFP are cloned in the direct (pHBRF) and reverse (pHBRR) orientation, while the plasmid pHBPR contains the full-length blue and green fluorescent protein encoding sequences.

RESULTS

We developed a transient transfection system to measure homologous recombination based on reactivation of Enhanced Green Fluorescent Protein (EGFP). The main features of the plasmid system are outlined in Fig. 1A. The plasmid harbors an intact blue-shifted EGFP sequence (EGFP), under control of a CMV promoter and with a SV40 polyadenylation signal. Compared with EGFP, EBFP has a Tyrosine at amino acid position 66 which creates a shift in the excitation and emission spectra that allows independent detection of EBFP from EGFP. In the experiments described here, the EBFP signal is used as a measure for transfection efficiency in each individual experiment. Also present in the plasmid is a chimeric sequence composed of *Aequorea victoria* GFP DNA in-frame with about 300 base pairs of the humanized EGFP sequence. The *A. victoria* part of this sequence contains amino acids

TABLE I

Properties of Human Tumor Cell Lines Studied

Cell line	Tissue	Genetic features
Saos-2	Osteosarcoma	Hypotriploid, p53 null
G292	Osteosarcoma	p53 null
HT1080		Near diploid, p53 wild-type
HT1080TG	Fibrosarcoma	p53 mutant (HT1080TG)
RKO	Colorectal carcinoma	Near diploid, p53 wild-type, mismatch repair deficient (MLH1 inactivated by methylation)
HCT116 HCT116 + 3	Colorectal carcinoma	Near diploid, p53 wild-type, mismatch repair deficient (MLH1) and proficient (MLH1 restored by chromosome 3 transfer)
A549	Lung carcinoma	Hypotriploid, p53 wild-type
Calu-1	Lung squamous cell carcinoma	Hypotriploid, p53 null
NCI-H520	Lung squamous cell carcinoma	Hypotriploid, p53 wild-type (33)
NCI-H661	Lung large cell carcinoma	Hyperhexaploid, p53 wild-type (33)
HCC1937	Breast carcinoma	Highly aneuploid (modal chromosome count 100), BRCA1 mutant, p53 mutant
Capan-1	Pancreatic carcinoma	Hypotriploid, BRCA2 and p53 mutant
DT40	Chicken lymphoma	High levels of homologous recombination

62–68, which make up the chromophore of GFP and determine the emission spectra. After 300 base pairs of EGFP sequence, the chimeric sequence provides a protein translation termination signal, which limits the size of the protein to the first 177 amino acids of the full-length 238 amino acids of EGFP. It was previously shown that all but the most terminal 7–10 amino acids are essential for green fluorescence (28). This means that the chimeric truncated GFP sequence should not yield any green fluorescence. Transfection experiments with the chimeric truncated GFP did not result in any green fluorescence when transfected into eukaryotic cells, but a full-length version of this chimeric GFP sequence did result in green fluorescence (data not shown). The chimeric and truncated GFP were cloned in two orientations into the recombination vector (Fig. 1B). The different orientation of the recombination partners within the plasmid may have implications for the mechanisms of HR that causes reactivation of GFP. The inter-molecular HR events are not expected to demonstrate any differences as a result of this orientation, but intra-molecular recombination may conceivably be affected. For instance, recombination of the inverted orientation of the GFP sequences is expected only by cross-overs, while the direct orientation may support single-strand annealing or replication slippage in addition to cross-overs.

To validate the properties of the homologous recombination system, we chose a panel of human tumor cell lines with known genetic defects, some of which involving different aspects of HR. Cell lines with wild-type and mutant p53 were selected because mutations in p53 are known to increase the levels of HR (10, 11). We selected cell lines with defects in BRCA1 or BRCA2, which were expected to have decreased levels of HR (12). DNA mismatch repair can affect HR, especially when the two recombination partners are not perfectly homologous. Another feature of DNA mismatch repair deficient cells is that they rarely show gross chromosomal abnormalities, but it is unknown if this is related to recombination repair (2). For these reasons, we also included cell lines with defects in DNA mismatch repair, including a cell line in which this defect was corrected by chromosome transfer (HCT116+3) (24). In addition, the panel includes several osteosarcoma cell lines, which have a high level of chromosomal abnormalities and which have a high frequency of p53 inactivation by genetic rearrangements. Table I lists the cell line panel and information on origin, chromosomal content, and known genetic defects.

The listed cell lines were transfected with the recombination plasmids and subjected to flow cytometric analysis as described in the methods section. An example of a flow cytometric analysis is shown in Fig. 2. The transfection efficiencies expressed as percentage of blue fluorescent cells of the total cell population varied between below detection levels (about 0.01%) to about 20%. The mean transfection efficiency values for each cell line are listed in Table II. Although the efficiencies varied within and between replicate experiments, the green/blue fluorescence ratios were mostly independent of this variation. In a few experiments and in the cell lines Capan-1 and DT40 the transfection efficiencies were extremely low, with the total number of blue fluorescent cells below 100. In these experiments the ratio of green/blue fluorescence became unreliable and so they were excluded as described in the methods.

The green/blue ratios for the forward and reverse constructs for each cell line is plotted in Fig. 3. Several observations can be made from these experiments. The reactivation of green fluorescence occurred at detectable levels in all cell lines tested, while the difference

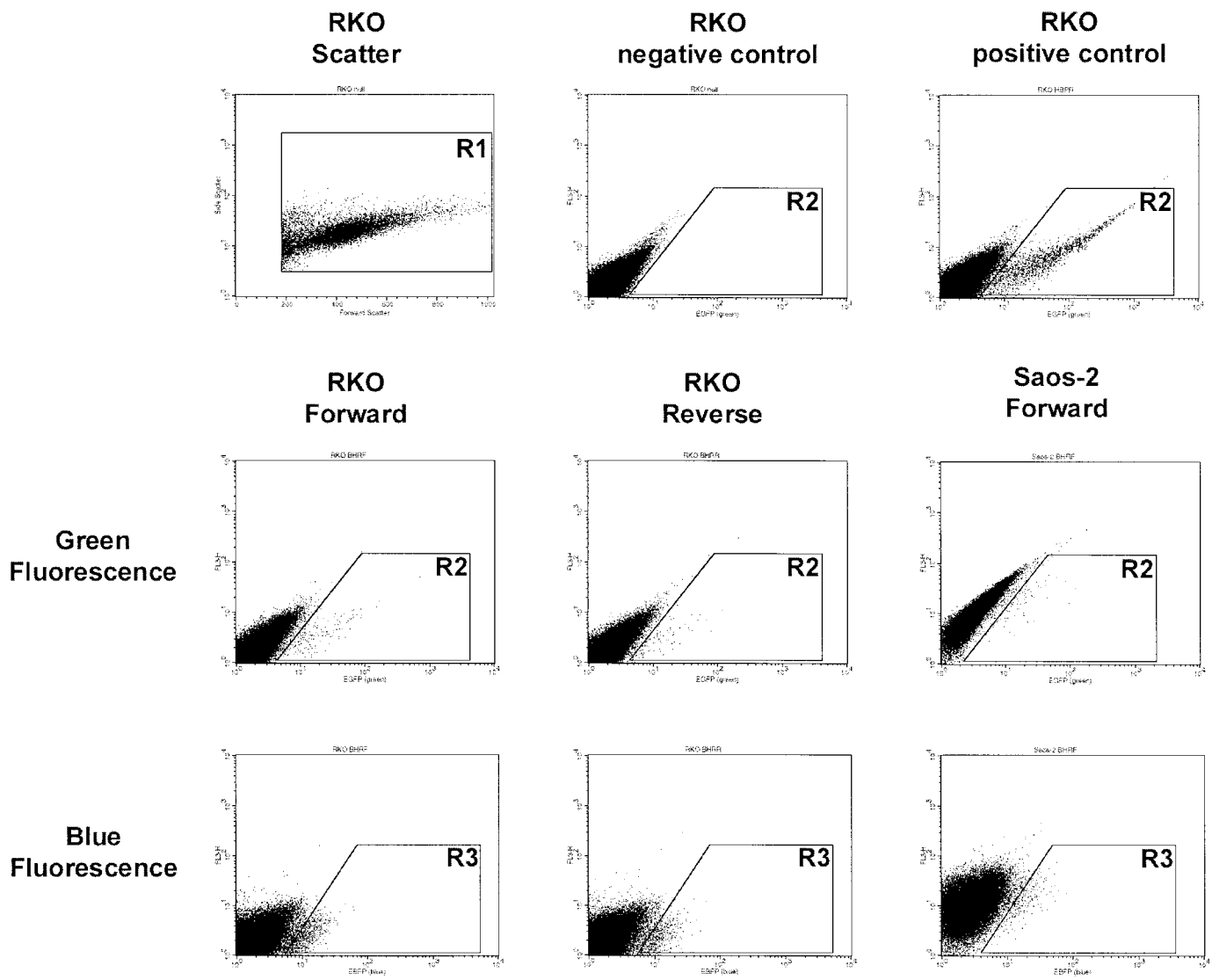

FIG. 2. Examples of flow cytometric analysis of green and blue fluorescent protein in human cell lines. The first row indicates the standard cellular features of forward and side-scatter indicating a viable cell population (left panel), the measurement of green fluorescent cells by ratio analysis with red fluorescence (middle panel), and green fluorescence measured with the positive control plasmid pHBPR (right panel). Measurements with the colorectal cell line RKO are shown for green (middle row) and blue (lower row) fluorescence using the forward plasmid pBHRF (left panels) and reverse plasmid pBHRR (middle panels), and the osteosarcoma cell line Saos-2 with the forward plasmid pBHRF (right panels).

in reactivation between the lowest and highest reactivating cell line was about 100-fold. The lowest levels were found in the BRCA1 mutant cell line HCC1937, which was expected to be impaired in HR capacity. When the results from both the forward and reverse plasmids were taken together, the reactivation ratio of HCC1937 cells was not significantly different from G292 cells and the HCT116 cell lines, borderline significantly different from A549 cells ($P = 0.05$, Student's *t* test), but highly significantly different from all other cell lines. To investigate a role of the mismatch repair system in HR we examined the mismatch repair deficient and proficient derivative HCT116 cell lines. The reactivation levels were not different between these cell lines, but both were about fivefold lower than the other cell line known to have a defect in DNA mismatch repair, the colorectal cell line RKO ($P < 0.001$, Student's *t* test). Reactivation levels in the forward oriented plasmid construct pHBRF were about 20-fold higher in the p53 mutant cell line HT1080TG compared with the parental p53 wild-type fibrosarcoma line HT1080, while this difference was about sixfold for the reverse oriented plasmid construct pHBRR. This difference was completely attributable to different reactivation levels in the p53 mutant line HT1080TG, and was statistically significant ($P < 0.001$, Student's

TABLE II

Transfection Efficiencies and Homologous Recombination Capacity of Human Tumor Cell Lines

Cell line	Transfection efficiency[a]	Ratio green/blue pHBRF (forward orientation)	Ratio green/blue pHBRR (reverse orientation)
Saos-2	510	0.20 (±0.06)[b]	0.33 (±0.13)
G292	1753	0.03 (±0.03)	0.09 (±0.06)
HT1080	1363	0.29 (±0.26)	0.51 (±0.42)
HT1080TG	153	5.42 (±0.68)	0.89 (±0.16)
RKO	637	0.73 (±0.39)	0.42 (±0.19)
HCT116	804	0.11 (±0.03)	0.08 (±0.02)
HCT116+3	3947	0.10 (±0.01)	0.05 (±0.01)
A549	1624	0.16 (±0.15)	0.08 (±0.03)
Calu-1	473	0.66 (±0.66)	0.41 (±0.33)
NCI-H520	141	0.15 (±0.10)	0.37 (±0.31)
NCI-H661	848	0.28 (±0.29)	0.16 (±0.11)
HCC1937	2363	0.05 (±0.04)	0.06 (±0.06)
Capan-1	<10	ND[c]	ND
DT40	<1	ND	ND

[a] Expressed as number of green fluorescent cells per 10^5 using the positive control plasmid pBHPR.
[b] Ratio green/blue with standard errors in parentheses.
[c] Not determined.

t-test). Two other cell lines with an apparent difference between the two plasmid constructs were the osteosarcoma cell line G292 and the lung carcinoma cell line H520, however, these differences were not statistically significant ($P = 0.17$ and $P = 0.13$, respectively, Student's *t*-test). Other cell-type specific characteristics such as chromosomal content (aneuploidy), cell type of origin, or p53 status did not correlate with increased or decreased HR capacity. The cell lines with pseudo diploid karyotypes had both high (HT1080 and RKO) and low (HCT116) reactivation ratios. Within each tumor type (sarcoma, colorectal, lung), high and low ratios were apparent, while the only breast cancer cell line had a known genetic defect in BRCA1. The status of the p53 tumor suppressor gene ranged from wild-type (HT1080, RKO, and HCT116), null (Saos-2, G292, H520), to mutant (HT1080TG, A549, HCC1937). Within each of these categories, cell lines with high and low reactivation ratios were present (Fig. 3).

DISCUSSION

DNA recombination is one of the major DNA repair mechanisms that determine genome organization and stability. In mammalian cells, recombination by nonhomologous end-joining (NHEJ) has long been considered the major pathway, but recently the importance of homologous recombination for the integrity of the human genome has become clear. For instance, a direct role of BRCA1 in HR was recently demonstrated, while

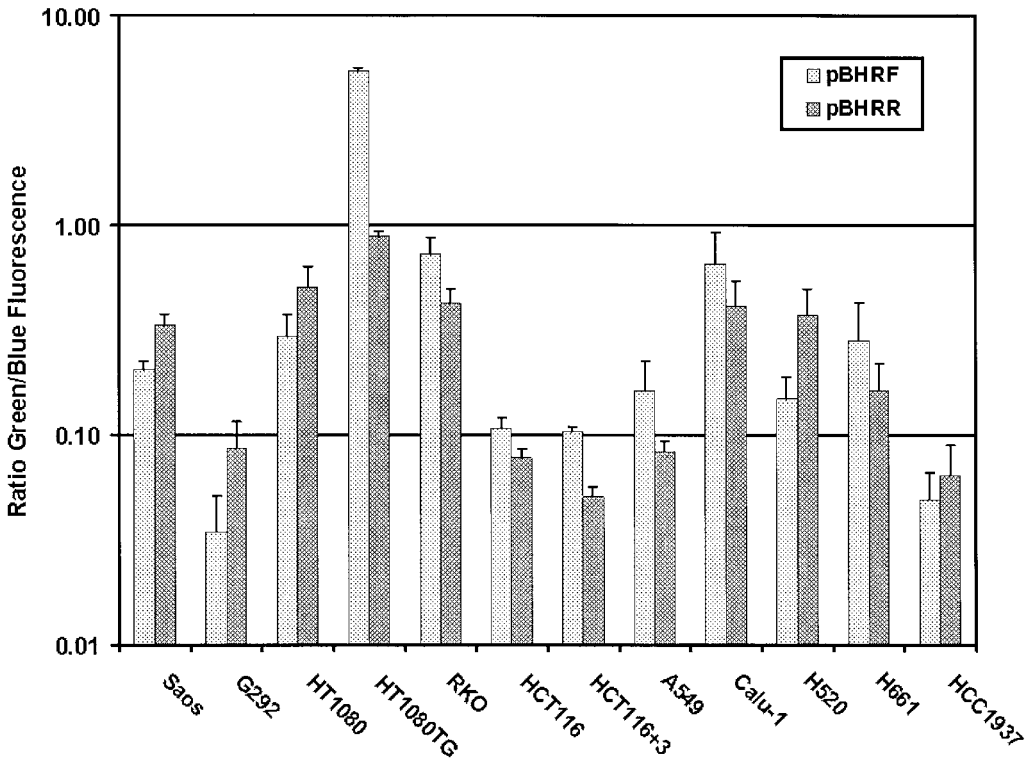

FIG. 3. Graphical representation of the observed ratios of green versus blue fluorescence in the panel of 12 human cell lines. The results of the forward and reverse plasmid constructs are shown separately with error bars indicating standard errors.

the p53 tumor suppressor inhibits HR under normal conditions (10–12). This link with cancer-associated genes suggests that proper control of DNA repair by HR is required to maintain chromosomal integrity, and that abnormal recombination repair may contribute to nuclear aneuploidy. In normal cells, HR is a high fidelity repair mechanism that is used to repair otherwise lethal DNA double-strand breaks (DSBs). It was recently shown that almost half of the DSBs induced by a specific endonuclease are repaired by HR (7). In fact, DNA DSBs are considered to be the most potent substrates for recombination repair. Defects in recombination repair may favor more error-prone DSB repair by, for instance, NHEJ. On the other hand, a large proportion of the human genome consists of repeated elements that form the potential for misalignment that can lead to gross rearrangements, loss of genetic information and genomic instability. The validity of this concept is demonstrated by the abnormally high levels of recombination seen in Ataxia Telangectasia cells that lead to chromosomal instability and increased risk for cancer in patients affected with this disorder (4).

The newly developed assay system for HR described here can be used as a direct measurement of HR events. The plasmid constructs harbor a 300 base pair stretch of perfect homology between an active blue shifted GFP and a truncated chimeric GFP. It was previously shown that perfectly homologous sequences over 200 base pairs in length can effectively drive HR (29). Our assay provides a rapid assessment of HR capability that can be used to compare recombination levels between different cell lines within days. Our results demonstrate plasmid reactivation through HR with a difference of at least 100-fold between cell lines tested in our panel. In addition, the sensitivity of the system is sufficient to measure the large effects of the inactivation of genes such as BRCA1 or p53.

The fact that we saw a difference between the forward and reverse plasmid orientations in HT1080TG cells indicates that there must be a significant level of intra-molecular recombination because the orientation of the recombination partners within the plasmid is not expected to make a difference to the level of inter-molecular events. Since this cell line is a p53 mutant derivative of HT1080 cells, these results suggest a role for p53 in the observed difference between the forward and reverse orientation of the homologous sequences. The possible recombination mechanisms that are expected to lead to reactivation of either sequence orientation are crossing-over and gene conversion. In addition, single-strand annealing or replication slippage could potentially repair the direct sequence orientation, while the reverse orientation would only be expected to support recombination repair. It is interesting to note that there is evidence for a role of p53 in the processing of strand exchange intermediates, structures that may resemble those associated with DNA cross-overs (30). It was previously suggested that defects in DNA mismatch repair can influence the levels of HR in a cell, especially under conditions of near perfect homology between the recombination partners (31). We did not observe any differences in an isogenic system with or without DNA mismatch repair defects, presumably because the homology between the GFP sequences is 100% in our construct and does not depend on this type of DNA repair for optimal alignment.

There are some limitations to the approach of a direct measurement of DNA recombination by green fluorescent protein. Flow cytometry for GFP and BFP only allows for the measurement of relative differences because of the possibility that only cells that have undergone multiple recombination events generate fluorescence levels above background. Related to this limitation is the need for sufficiently high transfection efficiencies to make reliable measurements. We chose to reject those experiments where less than 100 of the 50,000 analyzed cells demonstrated detectable blue fluorescence. This limitation excluded some cell lines with low transfection efficiencies such as the BRCA2 deficient pancreatic carcinoma cell line Capan-1, and the chicken lymphoma cell line DT40, which has very high levels of recombination (26).

It was previously shown that in liposome-based transfection methods, the number of plasmid molecules entering the cell can be as high as 10^5 to 10^6 (32). This finding has several implications. First, the abundant availability of homologous sequences may facilitate recombination events between separate plasmid molecules rather than intra-molecular events. And second, these high numbers of plasmid DNA copies may result in non-physiological conditions within the cell that may alter the final outcome of the results. This may work in favor of HR because the target sequence is readily available, but it may also have the opposite effect by diluting out the cellular proteins that are necessary to carry out the recombination steps. The above features also mean that we may not derive reliable recombination frequencies from the data obtained with this host-cell reactivation system.

In conclusion, we describe the development of a novel host cell reactivation system that can be used to measure HR in *in vitro* cultures of cell lines. The system was validated with a panel of human tumor cell lines with known defects in genes that have an influence on HR. The effects of mutations in p53 and BRCA1 were readily apparent using the reactivation plasmids. The differential effects of p53 status on recombination levels measured in plasmids with a forward and reverse orientation of the homologous sequences suggests a role of p53 in the processing of intra-molecular recombination events.

ACKNOWLEDGMENTS

The authors thank Dr. Carl Bortner for assistance with flow cytometry and Jill Kucab for technical support.

REFERENCES

1. Vessey, C. J., Norbury, C. J., and Hickson, I. D. (1999) *Prog. Nucleic Acid Res. Mol. Biol.* **63,** 189–221.
2. Lengauer, C., Kinzler, K. W., and Vogelstein, B. (1998) *Nature* **396,** 643–649.
3. Jasin, M. (2000) *Cancer Invest.* **18,** 78–86.
4. Morrison, C., Sonoda, E., Takao, N., Shinohara, A., Yamamoto, K., and Takeda, S. (2000) *EMBO J.* **19,** 463–471.
5. Critchlow, S. E., and Jackson, S. P. (1998) *Trends Biochem. Sci.* **23,** 394–398.
6. Richardson, C., and Jasin, M. (2000) *Nature* **405,** 697–700.
7. Liang, F., Han, M., Romanienko, P. J., and Jasin, M. (1998) *Proc. Natl. Acad. Sci. USA* **95,** 5172–5177.
8. Resnick, M. A., and Cox, B. S. (2000) *Mutat. Res.* **451,** 1–11.
9. Zhang, H., Tombline, G., and Weber, B. L. (1998) *Cell* **92,** 433–436.
10. Bertrand, P., Rouillard, D., Boulet, A., Levalois, C., Soussi, T., and Lopez, B. S. (1997) *Oncogene* **14,** 1117–1122.
11. Mekeel, K. L., Tang, W., Kachnic, L. A., Luo, C. M., DeFrank, J. S., and Powell, S. N. (1997) *Oncogene* **14,** 1847–1857.
12. Moynahan, M. E., Chiu, J. W., Koller, B. H., and Jasin, M. (1999) *Mol. Cell* **4,** 511–518.
13. Chen, J. J., Silver, D., Cantor, S., Livingston, D. M., and Scully, R. (1999) *Cancer Res.* **59,** 1752s–1756s.
14. Lane, D. P. (1992) *Nature* **358,** 15–16.
15. Willers, H., McCarthy, E. E., Wu, B., Wunsch, H., Tang, W., Taghian, D. G., Xia, F., and Powell, S. N. (2000) *Oncogene* **19,** 632–639.
16. Dudenhoffer, C., Kurth, M., Janus, F., Deppert, W., and Wiesmuller, L. (1999) *Oncogene* **18,** 5773–5784.
17. Sturzbecher, H. W., Donzelmann, B., Henning, W., Knippschild, U., and Buchhop, S. (1996) *EMBO J.* **15,** 1992–2002.
18. Marmorstein, L. Y., Ouchi, T., and Aaronson, S. A. (1998) *Proc. Natl. Acad. Sci. USA* **95,** 13869–13874.
19. Matsuda, M., Miyagawa, K., Takahashi, M., Fukuda, T., Kataoka, T., Asahara, T., Inui, H., Watatani, M., Yasutomi, M., Kamada, N., Dohi, K., and Kamiya, K. (1999) *Oncogene* **18,** 3427–3430.
20. Hiramoto, T., Nakanishi, T., Sumiyoshi, T., Fukuda, T., Matsuura, S., Tauchi, H., Komatsu, K., Shibasaki, Y., Inui, H., Watatani, M., Yasutomi, M., Sumii, K., Kajiyama, G., Kamada, N., Miyagawa, K., and Kamiya, K. (1999) *Oncogene* **18,** 3422–3426.
21. Kucherlapati, R. S., Eves, E. M., Song, K. Y., Morse, B. S., and Smithies, O. (1984) *Proc. Natl. Acad. Sci. USA* **81,** 3153–3157.
22. Subramani, S., and Berg, P. (1983) *Mol. Cell Biol.* **3,** 1040–1052.
23. Thyagarajan, B., McCormick-Graham, M., Romero, D. P., and Campbell, C. (1996) *Nucleic Acids Res.* **24,** 4084–4091.
24. Koi, M., Umar, A., Chauhan, D. P., Cherian, S. P., Carethers, J. M., Kunkel, T. A., and Boland, C. R. (1994) *Cancer Res.* **54,** 4308–4312.
25. Anderson, M. J., Casey, G., Fasching, C. L., and Stanbridge, E. J. (1994) *Genes Chromosomes Cancer* **9,** 266–281.
26. Koi, M., Lamb, P. W., Filatov, L., Feinberg, A. P., and Barrett, J. C. (1997) *Cytogenet. Cell Genet.* **76,** 72–76.
27. Pierce, A. J., Johnson, R. D., Thompson, L. H., and Jasin, M. (1999) *Genes Dev.* **13,** 2633–2638.
28. Li, X., Zhang, G., Ngo, N., Zhao, X., Kain, S. R., and Huang, C. C. (1997) *J. Biol. Chem.* **272,** 28545–28549.
29. Rubnitz, J., and Subramani, S. (1984) *Mol. Cell Biol.* **4,** 2253–2258.
30. Susse, S., Janz, C., Janus, F., Deppert, W., and Wiesmuller, L. (2000) *Oncogene* **19,** 4500–4512.
31. Ciotta, C., Ceccotti, S., Aquilina, G., Humbert, O., Palombo, F., Jiricny, J., and Bignami, M. (1998) *J. Mol. Biol.* **276,** 705–719.
32. Tseng, W. C., Haselton, F. R., and Giorgio, T. D. (1997) *J. Biol. Chem.* **272,** 25641–25647.
33. Stoler, D. L., Chen, N., Basik, M., Kahlenberg, M. S., Rodriguez-Bigas, M. A., Petrelli, N. J., and Anderson, G. R. (1999) *Proc. Natl. Acad. Sci. USA* **96,** 15121–15126.